NACA RM L56E09

NACA

RESEARCH MEMORANDUM

EXPERIMENTAL INVESTIGATION OF THE EFFECT OF BOUNDARY-LAYER TRANSITION ON THE AVERAGE HEAT TRANSFER TO A YAWED CYLINDER IN SUPERSONIC FLOW

By Ivan E. Beckwith and James J. Gallagher

Langley Aeronautical Laboratory
Langley Field, Va.

NATIONAL ADVISORY COMMITTEE
FOR AERONAUTICS

WASHINGTON

July 13, 1956

Declassified September 1, 1959

NACA RM L56E09

NATIONAL ADVISORY COMMITTEE FOR AERONAUTICS

RESEARCH MEMORANDUM

EXPERIMENTAL INVESTIGATION OF THE EFFECT OF BOUNDARY-LAYER TRANSITION ON THE AVERAGE HEAT TRANSFER TO A YAWED CYLINDER IN SUPERSONIC FLOW

By Ivan E. Beckwith and James J. Gallagher

SUMMARY

The average heat-transfer to the forward half of a circular cylinder was measured in a blowdown jet at a stream Mach number of 4.15. The test Reynolds number based on the diameter of the cylinder was varied from 5×10^5 to 13×10^5 and the yaw angle was varied from 0° to 60°. Most of the tests were made at a wall-to-stagnation temperature ratio of about 0.8.

The test results showed that, as the yaw angle was increased from 0° to 35°, the average heat-transfer coefficient increased by 50 percent at a Reynolds number of 5×10^5, and at a Reynolds number of 13×10^5 the heat-transfer coefficient increased by 100 percent. Comparison of the measured heat-transfer coefficients with theoretical predictions and with other experimental results indicated that these large increases in heat transfer, with increasing yaw angle and fixed Reynolds number, were caused by transition from laminar to turbulent boundary layer. This transition apparently occurred primarily as a result of a dynamic type of instability which is associated with the secondary flow in the boundary layer on the yawed cylinder.

Further increase of the yaw angle from 35° to 60° resulted in a reduction in the average heat-transfer coefficients of about 35 percent from the peak values. Most of this reduction apparently corresponds to the decrease in heat transfer with increasing yaw angle that could be expected to occur on a cylinder with a completely developed turbulent boundary layer.

INTRODUCTION

The use of sharp leading edges on wings and tail surfaces is undesirable at flight speeds for which aerodynamic heating becomes a serious problem because of the high local heat-transfer coefficients and small heat capacity of the sharp edge. Both of these difficulties can be alleviated by using a blunt leading edge. Blunting the leading edge, however, has the disadvantage of increasing the drag. The increased drag of the blunted section can be reduced by increasing the sweepback angle of the wing. For these reasons, data are needed on the effects of sweepback on the heat transfer to blunt leading edges.

A yawed cylinder of high aspect ratio conveniently simulates the leading edge of a sweptback wing and also allows a simplified treatment of the theoretical problem. Thus, for incompressible flow with a Prandtl number of 1, inspection of the laminar-boundary-layer equations for the infinite yawed cylinder (refs. 1 and 2) shows that the velocity distribution in planes normal to the cylinder axis and the heat transfer depend only on the flow component normal to the cylinder. Solutions for this case (refs. 3 and 4) then show that the local Nusselt number, based on cylinder chord measured normal to the leading edge, is proportional to the square root of a Reynolds number based on the chordwise component of the stream velocity and the normal chord. That is to say, for fixed stream conditions and fixed normal chord, the heat-transfer coefficient is proportional to the square root of the cosine of the yaw angle. Application of these results to a wing of fixed cross-sectional shape, planform area, and normal chord indicates that, for given stream conditions and wall temperature, the total quantity of heat transferred to the wing is also proportional to the square root of the cosine of the sweepback angle.

The results of theoretical and experimental investigations made at supersonic speeds (refs. 5 to 8) show that, for laminar boundary layers, somewhat larger reductions in heat transfer can be obtained by yawing the cylinder than would be expected for the corresponding incompressible-flow case. This is largely because of the effect of the detached bow wave on the local flow conditions near the cylinder. Apparently, then, as long as the boundary layer remains laminar, some reduction in total heat transfer to a wing and its leading edge is to be expected by increasing the sweepback angle. It could also be expected that, as the flight Reynolds number is increased, transition from laminar to turbulent flow will eventually occur and cause the associated large increases in heat-transfer rates.

A related phenomenon, which is probably not so generally appreciated, is the effect of the sweepback or yaw itself on transition. Recent investigations (refs. 9 to 13 and papers of limited availability by the British investigators P. R. Owen and D. G. Randall) have shown that sweepback or

yaw has large adverse effects on transition on a wing or cylinder. Owen and Randall have shown that these effects are caused by a dynamic type of instability which arises as a result of the secondary or three-dimensional flow that occurs within the boundary layer on a sweptback wing or cylinder. They also defined and, from experimental data, evaluated a stability parameter which has been successfully applied to the calculation of a lower limit of Reynolds number and yaw angle at which this instability first appears for incompressible flow. The results of reference 12 indicate that this instability may appear at a much lower Reynolds number on a wing in supersonic flow than predicted by the Owen-Randall parameter for incompressible flow.

The purpose of the present report is to present data showing the effect of yaw on the heat transfer to cylinders over a higher Reynolds number range than that of previous data. The Reynolds number range of the present tests, based on free-stream conditions and cylinder diameter, is from 5×10^5 to 13×10^5. This corresponds to flight conditions at altitudes of 45,000 to 62,000 feet at a Mach number of 4 with a wing leading-edge radius of 1 inch. The data are compared with correlation parameters for laminar and turbulent heat transfer and also with laminar-heat-transfer data from previous investigations. Estimated values of the transitional Reynolds numbers from the present investigation are compared with values predicted by the Owen-Randall stability parameter evaluated from the data of reference 9.

SYMBOLS

A	cross-sectional area of model
C	constant in equation (14)
C_1, C_2	constants in equation (10)
C_p	"normal" pressure coefficient
c	specific heat of model material
c_p	specific heat of air
D	diameter of model
h	heat-transfer coefficient
k	thermal conductivity of air

k_m	thermal conductivity of model material
k', μ'	reference conductivity and viscosity evaluated at T'
L	length from leading edge or stagnation point along an external streamline
l	spanwise length of model
M	Mach number
M_N	normal component of Mach number ahead of cylinder
M_l	local chordwise component of Mach number
Nu	Nusselt number
P	periphery of model exposed to stream
p	pressure
q_w	convective heat-transfer rate per unit area at the surface
R	Reynolds number
r	recovery factor
T	temperature, $^{\circ}R$
T_e	equilibrium temperature, $^{\circ}R$
T'	reference temperature, $\frac{1}{2}\left(T_s + T_w\right)$
t	time
U	resultant velocity ahead of cylinder
U_N	normal component of velocity ahead of cylinder
u	local chordwise velocity
V	local resultant velocity
v	local velocity component normal to external streamline

x distance from stagnation point along the surface of the cylinder in a plane normal to the leading edge

$\bar{x} = \frac{x}{D}$

y distance measured along span of model

z boundary-layer coordinate normal to surface

γ ratio of specific heats

Δ boundary-layer momentum thickness

δ boundary-layer thickness

θ angular distance around cylinder measured from stagnation line

λ Pohlhausen boundary-layer parameter, $\frac{\rho \frac{du_1}{dx} \delta^2}{\mu}$

μ dynamic viscosity of air

ρ mass density of air

ρ' reference density, $\frac{1}{2}\left(1 + \frac{T_s}{T_w}\right)\rho_s$

σ Prandtl number

τ shear stress

χ stability parameter

ψ angle of yaw (acute angle between the spanwise axis of the model and the plane perpendicular to the free-stream flow direction)

ω specific weight of model material

Subscripts:

D based on D

L based on L

1	local value external to boundary layer
o	at stagnation line of cylinder
s	just behind bow shock
T	at transition
t	stagnation value as determined by isentropic deceleration of flow external to boundary layer
w	at wall on surface of model
max	maximum
Δ	based on Δ
∞	in free stream ahead of bow shock

Superscript:

'	evaluated at reference quantities T' and ρ'

A bar over a symbol denotes the average value over the forward half of the cylinder unless otherwise noted.

APPARATUS

Description of Tunnel

The investigation was made in a blowdown jet in the Gas Dynamics Branch at the Langley Laboratory. The test section is 12 inches wide and 13 inches high. The complete system consists of a high-pressure settling chamber, a convergent-divergent nozzle, a pressure-tight chamber containing the model support system, and a fixed diffuser. The stagnation temperature and pressure are controlled automatically at a remote station.

The air supply is obtained from tanks where the air is stored at a maximum pressure of 5,000 pounds per square inch. The air is reduced in pressure by two successive regulating stations to the desired stagnation pressure, which was between 200 and 500 pounds per square inch for this investigation. The specific humidity of the air was less than 1 part of water per million parts of air by weight. The air is heated by a combination of a Dowtherm heat exchanger and electric heaters. The maximum stagnation temperature which can be attained is 1,040° F; however, for this investigation the highest temperature was limited to about 400° F and the maximum variation of the stagnation temperature with time

was limited to 1° F per minute. The maximum running time available for this particular blowdown jet is from 20 to 40 minutes, depending on stagnation conditions.

Mach number distributions, as obtained from total-pressure surveys made in a horizontal plane 1/4 inch above the nozzle center line, are presented in figure 1. This figure shows a slight variation in Mach number in the test region; however, no large disturbances appear. The average Mach number is 4.15 with a maximum variation of ±0.03 over most of the test region.

Models

The heat-transfer model was a 24-inch-long cylinder made of electrolytic pure copper. The cross-sectional shape of the cylinder was a semicircle of 1/2-inch diameter. The model was supported in the test section by a steel bar with the leading edge grooved out to reduce heat conduction between the model and its support bar. A sketch of the model and its support is shown in figure 2(b). The model was fastened to and alined with the support by means of small screws and pins. The space between the model and the edges of the support was sealed with a polysulfide rubber.

The model was covered and water-cooled by means of a shield (fig. 2) during the transient starting conditions. The shield covered the model until equilibrium conditions were established in the test section, and then it was rapidly retracted by a cable attached to a pneumatic cylinder. The removal time was less than 0.01 second.

The model was provided with end plates (fig. 2) in order to minimize aerodynamic end effects. The upstream end plate was attached to the model and the downstream end plate was attached to the shield. The clearance between the model and the shield in the retracted position was filled by a contoured block attached to the model. This provided a smooth end plate during the time that temperature data were recorded. Slots were cut into the model near each end plate and filled with an insulating material to minimize heat conduction at the ends of the model. The end plates were parallel to the tunnel sidewalls and $1\frac{1}{2}$ inches from them for all the yaw angles tested. The aspect ratio of the model (between the end plates) thus varied with the yaw angle according to the relation

$$\frac{l}{D} = \frac{18}{\cos \psi}$$

The temperature of the model was measured by copper constantan thermocouples which were silver-soldered to the rear of the model as

shown in figure 2(b). The thermocouples were spaced 1 inch apart along the span of the model. Eleven thermocouples were used so that longitudinal heat conduction and aerodynamic end effects (if any) could be evaluated. The model was located in the blowdown jet so that the center thermocouple was at station 0 in the nozzle (see fig. 1) for all yaw angles except 0°, for which the model was $4\frac{1}{2}$ inches farther down the tunnel.

Two pressure-distribution models were used to obtain data at 0° and 45° yaw. These models were complete circular cylinders and had end plates similar to those of the heat-transfer model. The aspect ratios between the end plates were 4 and 14, respectively. Pressure orifices were installed at intervals of 5° over the first 40° and thereafter at intervals of 10° and 15°.

Instrumentation

The temperature time history of the model was obtained from a 36-channel recording oscillograph having elements with a sensitivity of 12.8 microamperes per inch of deflection. The elements were so positioned that $1\frac{1}{2}$ inches of deflection was obtained. This corresponded to a rise of 250° F above cold junction temperature. The galvanometer elements were individually calibrated before each run, giving an accuracy in absolute temperature of 1° F. However, on the temperature-time records for any one channel, the relative temperatures were accurate to within 1/4° F.

The stagnation temperature was obtained from a self-balancing recording potentiometer. Measurements were made with three thermocouples installed in the settling chamber. The stagnation temperature is accurate to within ±2° F. Stagnation pressure was measured on a Bourdon gage accurate to ±2 pounds per square inch. The stagnation temperature and pressure were also recorded on the oscillograph to coordinate them with the temperature time history of the model.

TEST PROCEDURE AND DATA REDUCTION

Heat-Transfer and Recovery-Temperature Tests

The piping system, tunnel, and nozzle were preheated at subsonic flow rates, for a period of about 2 hours prior to each test, until the inside wall temperatures of the nozzle were up to about 95 percent of absolute stagnation temperature. Immediately after the desired preheat

temperature was attained, the supersonic run was started. When the tunnel stagnation conditions reached steady values (after 15 to 20 seconds) the model shield was retracted and the cooling water was simultaneously cut off. The oscillograph records showed that the film of water left on the model after retraction of the shield was evaporated in less than 0.1 second. The end of this time interval was taken as "time zero" for the model temperature time history. Sufficiently large water flow rates were used so as to insure a uniform temperature distribution along the model span at time zero. A typical time history of the model temperatures is shown in figure 3.

Recovery temperatures were obtained directly from test data by continuing the run until the recorded model temperatures reached a constant value. This required from 2 to 3 minutes running time, depending on the stagnation conditions.

Data Reduction

The equation for the average heat-transfer rate per unit surface area to a slender cylinder is

$$\bar{q}_w \equiv \bar{h}\left(\bar{T}_w - \bar{T}_e\right) = -\frac{\omega c A}{P}\frac{\partial \bar{T}}{\partial t} + \frac{k_m A}{P}\frac{\partial^2 \bar{T}}{\partial y^2} \qquad (1)$$

The temperature derivatives normal to the cylinder axis have been neglected so that $\bar{T}$ would be some effective mean temperature at any cross section. For this investigation, however, the heat-transfer coefficient was evaluated simply by using the measured temperatures for both $\bar{T}$ and $\bar{T}_w$ in equation (1). Since the thermocouples were located on the back of the model, lower indicated heat-transfer coefficients for small times would be obtained than if the actual mean temperatures and wall temperatures had been measured. By using available solutions for unsteady heat transfer to cylinders with a uniform heat-transfer coefficient at the surface (ref. 14), the error in heat-transfer coefficients due to thermocouple location was estimated to be between 1 to 2 percent for all heating rates encountered in the present investigation, even at the small times at which the data were reduced. For the half-cylinder model used in this investigation, $\frac{A}{P} = \frac{D}{4}$. The values for the thermal properties of copper were taken from reference 15, p. 268.

The last term on the right in equation (1) represents the net heat transfer due to spanwise heat conduction. Since this depends on the second derivative of an experimental quantity, it is difficult to evaluate accurately. Consequently, heat-transfer rates were calculated from the data at small times only, when spanwise temperature variations were

small and the temperature variation with time was large. All heat-transfer data presented are for times of less than 4 seconds from time zero. For this time interval, the largest value of the conduction term for any run was found to be only 3 percent of the total heat input, so that, in general, the conduction was neglected. Estimates showed that the quantity of heat contributed by radiation was also negligible compared with the storage term. The time-temperature slopes were read directly from plots such as shown in figure 3(b).

The mean equilibrium temperature $\overline{T}_e$ was taken as the arithmetic average of the measured temperatures for the condition of $\frac{\partial T}{\partial t} = 0$. This occurred after 2 to 3 minutes from time zero, depending on the stagnation conditions. Radiation was again found to be negligible since the tunnel wall temperatures were close to model equilibrium temperatures because of the preheating procedure.

THEORETICAL CORRELATION EQUATIONS

Laminar Boundary Layer

Approximate correlation equations for the heat transfer to yawed cylinders can be derived in a general form by the method of reference 8. The method is applied here to the forward half of a circular cylinder.

The average heat-transfer coefficient can be written as

$$\overline{h} = \frac{\overline{h}}{h_o} \frac{q_{w_o}}{T_w - T_{e_o}}$$

The substitution of the expression for $\frac{q_{w_o}}{T_w - T_{e_o}}$ obtained from equation (46) of reference 8 results in a general relation for the average Nusselt number,

$$\frac{\overline{h}D}{k_w} = \frac{\overline{h}}{h_o}\left[\frac{\rho_\infty U_\infty D}{\mu_w} \cos\psi \left(\frac{d}{d\bar{x}} \frac{u_1}{U_{N_s}}\right)_{x=0} \frac{\rho_{1_o}}{\rho_s}\right]^{1/2} \left[\frac{0.84}{\left(\frac{T_w}{T_{1_o}}\right)^{0.3}} - 0.4\right] \qquad (2)$$

The ratio $\bar{h}/h_o$ for the forward half of a circular cylinder has been evaluated by the method of reference 8 for $M_\infty = 4.1$ with $\frac{dT_w}{dx} = 0$. The local flow distributions needed for these calculations were obtained from the measured pressure distributions shown in figure 4 and from the assumptions that the flow outside the boundary layer is isentropic and independent of the spanwise flow. The local equilibrium temperature was taken as

$$\frac{T_e}{T_t} = \sqrt{\sigma} + \left(1 - \sqrt{\sigma}\right) \frac{T_{l_o}}{T_t} \frac{T_l}{T_{l_o}} \tag{3}$$

where

$$\frac{T_{l_o}}{T_t} = \frac{1 + \frac{\gamma - 1}{2} M_\infty^2 \cos^2\psi}{1 + \frac{\gamma - 1}{2} M_\infty^2} \tag{4}$$

The results of these calculations are shown in figure 5 where the ratio $\bar{h}/h_o$ is plotted against ψ for different values of T_w/T_t. The corresponding theoretical results from reference 8 for $M_\infty = 6.9$ and the experimental values from reference 6 for $M_\infty = 3.9$ are also shown in this figure for comparison. According to the method of reference 8 and the data of reference 6, the value of $\bar{h}/h_o$ on a circular cylinder is practically independent of T_w/T_t, M_∞, and ψ, as indicated in figure 5.

The mean equilibrium temperature $\bar{T}_e$ can be evaluated from equation (54) of reference 8 after noting that

$$\frac{4}{\pi} \int_0^{\pi/4} \frac{T_l}{T_{l_o}} d\bar{x} \approx 0.81 \tag{5}$$

to an accuracy of 2 percent over a large range of M_∞. The reason for this is that the value of M_l at any given value of $\bar{x}$ does not vary much with M_∞ or ψ. (See ref. 8.) Thus, to the degree of approximation in the theory,

$$\frac{\bar{T}_e}{T_t} = \sqrt{\sigma} + 0.81\left(1 - \sqrt{\sigma}\right) \frac{T_{l_o}}{T_t} \tag{6}$$

Then from equations (2) and (6) and from figure 5, the heat transfer to the front half of a circular cylinder can be easily calculated for a large range of stream Mach numbers, yaw angles, and temperatures.

Turbulent Boundary Layer

Detailed calculations for the local heat transfer to cylinders with turbulent boundary layers are possible by various approximate methods. (See, for example, refs. 16 and 17.) These methods involve the use of the integral momentum and energy equations together with somewhat arbitrary assumptions for the velocity and temperature profiles, skin-friction coefficients, and Reynolds analogy. The assumptions are usually concerned with the extension of low-speed results on the flat plate to higher speeds and/or arbitrary pressure gradients. In some cases, however, the skin friction and heat transfer may be evaluated from established equations for low-speed flow without the necessity of extensive calculations. Thus, for example, the expression for the skin friction on a flat plate in incompressible flow may be extended to supersonic flow with heat transfer by evaluating the gas properties at some reference temperature T' (ref. 18). The heat-transfer coefficient may then be evaluated directly from Reynolds analogy.

The Reynolds analogy cannot, of course, be used for the calculation of local heat-transfer coefficients on a cylinder with a blunt leading edge since the local chordwise shear stress is zero at the stagnation point. Also, the boundary layer would, presumably, always be laminar for at least some small distance downstream of the stagnation point. However, if the average heat-transfer coefficient is desired, as in the present tests, some form of Reynolds analogy can be used, and it should be possible to derive simple correlating equations.

The expression for the average skin friction over the chordwise distance x on a cylinder in incompressible flow is assumed to be of the form

$$\frac{\bar{\tau}_w}{\rho U_\infty^2} = \frac{C_1}{\left(\frac{\rho U_\infty x}{\mu}\right)^{1/7}} \tag{7}$$

where C_1 is a constant. For a flat plate, $C_1 \approx 0.015$ (ref. 19). The Reynolds analogy in terms of the average heat-transfer coefficient and average shear stress is assumed to be of the form

$$\frac{\bar{h}}{\rho U_\infty c_p} = C_2 \frac{\bar{\tau}_w}{\rho U_\infty^2} \tag{8}$$

For a flat plate and Prandtl number of 0.70, $C_2 = 1.2$ (ref. 20). Combining equations (7) and (8) then gives an expression for the average Nusselt number, which is

$$\frac{\bar{h}x}{k} = C_1 C_2 \sigma \left(\frac{\rho U_\infty x}{\mu} \right)^{6/7} \tag{9}$$

This result may be extended to compressible flow by evaluating all gas properties at some reference temperature T', which is defined here as simply

$$T' = \frac{1}{2}\left(T_s + \bar{T}_w \right)$$

The reference density ρ' is also taken as the average value

$$\rho' = \frac{1}{2}\left(\rho_s + \bar{\rho}_w \right)$$

which can be simplified to

$$\frac{\rho'}{\rho_s} = \frac{1}{2}\left(1 + \frac{\bar{p}_1}{p_s} \frac{T_s}{\bar{T}_w} \right) \approx \frac{1}{2}\left(1 + \frac{T_s}{\bar{T}_w} \right)$$

by noting that $\bar{p}_w = \bar{p}_1$ and that $\bar{p}_1 \approx p_s$ over the forward section of a cylinder. The reference velocity U_∞ in equation (9) would properly be some velocity behind the bow wave in supersonic flow. Then, assuming that to the first order of approximation the heat transfer is independent of the spanwise flow, the reference velocity U_∞ would have to be the normal velocity component behind the shock U_{N_s}. Equation (9) then becomes

$$\frac{\bar{h}x}{k'} \approx C_1 C_2 \sigma \left(\frac{\rho' U_{N_s} x}{\mu'} \right)^{6/7}$$

or, with $\frac{x}{D} = \frac{\pi}{4}$ on the forward half of a circular cylinder, the final result would be written as

$$\frac{\bar{h}D}{k'} \approx C_1 C_2 \sigma \left(\frac{\rho' U_{N_s} D}{\mu'} \right)^{6/7} \tag{10}$$

Hilpert (ref. 15, p. 142) has used an equation of this form for the average heat transfer to tubes in a cross flow.

The average recovery temperature $\bar{T}_e$ for a turbulent boundary layer may be calculated by assuming that the local recovery factor r is given by the expression

$$r = \sigma^{1/3} = \frac{T_e - T_l}{T_t - T_l}$$

Then, for the half-cylinder,

$$\frac{\bar{T}_e}{T_t} = \frac{4}{\pi}\int_0^{\pi/4} \frac{T_e}{T_t}\,dx = \sigma^{1/3} + 0.81\left(1 - \sigma^{1/3}\right)\frac{T_{l_o}}{T_t} \qquad (11)$$

by analogy with equation (6).

RESULTS AND DISCUSSION

Pressure Distributions

The results of the pressure-distribution tests are given in figure 4, where the "normal" pressure coefficient defined as

$$C_p = \frac{2}{\gamma M_{N_\infty}^2}\left(\frac{p_l}{p_\infty} - 1\right)$$

is plotted against θ. Data were obtained at $M_\infty = 1.98$ for $\psi = 0^\circ$ and at $M_\infty = 4.08$ for $\psi = 0^\circ$ and $\psi = 44.7^\circ$. The data at $M_\infty = 4.08$ were obtained in the same nozzle described in the section entitled "Apparatus" but at a time when the throat spacing of the nozzle was slightly different than that used in the heat-transfer tests for which the average stream Mach number M_∞ was 4.15 (see fig. 1). The $M_\infty = 1.98$ data were obtained in one of the other blowdown jets in the Langley Gas Dynamics Branch. Figure 4 shows that the normal pressure coefficient increases with increasing normal Mach number $\left(M_{N_\infty} = M_\infty \cos\psi\right)$ over the entire surface of the cylinder.

The dashed lines in figure 4 were computed from a modified Newtonian equation for the pressure coefficient (ref. 21),

$$C_p = C_{p_o} \cos^2\theta$$

where

$$C_{p_o} = \frac{2}{\gamma M_{N_\infty}^2}\left(\frac{p_{1_o}}{p_\infty} - 1\right)$$

with p_{1_o}/p_∞ taken as the theoretical pressure ratio across a normal shock at the Mach number M_{N_∞}. Since the data are in good agreement with the Newtonian equation, this equation is used (as in ref. 8) for calculating the velocity gradient at the stagnation line $\left(\frac{d}{d\bar{x}}\frac{u_1}{U_{N_s}}\right)_{x=0}$ which is required in equation (2). The experimental values of $\left(\frac{d}{d\bar{x}}\frac{u_1}{U_{N_s}}\right)_{x=0}$ shown in reference 8 were derived from the same data shown in figure 4.

Heat Transfer and Recovery Temperatures

The measured heat-transfer coefficients are presented in figure 6 in the form of a "wall" Nusselt number plotted against a Reynolds number. Each experimental point shown represents an average taken over the time interval from 1/2 second to 4 seconds from time zero for 3 or 4 representative stations along the span of the model. The values for the thermal conductivity and viscosity of air were taken from references 15 and 22, respectively. The wall temperatures for all the data were within the range of 90° F to 120° F so that most of the variation in T_w/T_t was obtained by changing T_t. The stream Reynolds number $\rho_\infty U_\infty D/\mu_\infty$ was varied from 5×10^5 to 13×10^5, corresponding to a maximum variation in the wall Reynolds number $\rho_\infty U_\infty D/\mu_w$ of 1.8×10^5 to 4×10^5. Data were obtained at the yaw angles of 0°, 21.0°, 39.7°, 49.3°, and 58.5°. The theoretical variation of $\bar{h}D/k_w$ with $\rho_\infty U_\infty D/\mu_w$ for laminar heat transfer according to equation (2) (with $\bar{h}/h_o = 0.67$) is also plotted in figure 6 for these same yaw angles.

Comparison of the data with this theory shows that at zero yaw angle the experimental Nusselt numbers are in good agreement with the theoretical values, while at all other yaw angles the experimental results are considerably higher than the theory and the differences between theory and experiment increase as the yaw angle and Reynolds number are increased. At zero yaw the effect of T_w/T_t on $\bar{h}D/k_w$, as predicted by equation 2 is in good agreement with the data except above a Reynolds number of 3×10^5 where the data are 5 percent to 8 percent higher than the theory.

The experimental recovery temperatures are shown in figure 7 as the ratio of the measured equilibrium temperature to the stagnation temperature plotted against yaw angle. Each point is the average of several temperatures measured along the model when the indicated variation of temperature with time was negligible. At zero yaw the data are in close agreement with the value predicted by equation (6) for a laminar boundary layer. As the yaw angle is increased, the data tend to approach the line from equation (11) for a turbulent boundary layer. While no definite conclusions can be obtained from figure 7 because of the limited accuracy of the data and theory, the trends suggest the possibility that the increase in heat-transfer coefficients with increasing yaw angles as shown in figure 6 is caused by transition to turbulent flow.

In order to explore this possibility, all the data are plotted in figure 8 in terms of the turbulent correlation parameters Nu' and R' as defined in equation (10). Laminar heat-transfer data from references 5 and 6, converted to these parameters, are also included in this figure. These two sets of data (excluding data from reference 5 at the higher yaw angles where end effects may be present), together with the theoretical values for laminar heat transfer as computed from equation (2), correlate with the data from the present tests for zero yaw. This indicates that the heat-transfer data of the present tests at zero yaw are laminar. Then, since the data at 21° yaw show the usual trend of transitional heat-transfer data, the increases in heat transfer with yaw angle in figure 6 are apparently caused by transition to turbulent flow and a forward movement of the transition region toward the stagnation line. Also, since the data at yaw angles from 39.7° to 58.5° correlate on one line with the slope given by equation (10), the transition has apparently reached its maximum forward position at about 40° yaw. That is, in effect, a completely developed turbulent boundary layer occurred on the cylinder for 40° to 60° yaw. Note that the product $C_1C_2\sigma = 0.024$, as obtained from the experimental results for ψ greater than 40°, is about 90 percent higher than the flat-plate value of 0.013.

Comparison of the present data with Hilpert's data (cited in ref. 15, p. 142), which is for the average heat transfer to a whole cylinder at zero yaw angle in subsonic flow, shows that at corresponding values of R' his data are between the laminar and turbulent values shown in figure 8. This can apparently be explained on the basis of the variation in local heat-transfer coefficient around a cylinder in subsonic flow as measured by Schmidt and Wenner (cited in ref. 15, p. 141). Examination of their data shows that, for subcritical Reynolds numbers, the contribution to the total heat transfer from the back of the cylinder is about the same as the contribution from the front. Hence, for subcritical Reynolds numbers, the average heat-transfer coefficient for the whole cylinder would be about the same as the average on the front. As the Reynolds number is increased, the heat contributed from the back increases rapidly in proportion to the contribution from the front since the heat transfer on the

front is apparently still laminar. Thus, for supercritical Reynolds numbers, the average heat transfer for the whole cylinder is greater than the average on the front. Consequently, for supercritical Reynolds numbers, the values of Nu' from Hilpert's data might be expected to fall between the laminar and turbulent values obtained in the present tests.

The relative magnitude of the increases in heat transfer with yaw angle for the present data is shown in figure 9, where the ratio of the average heat-transfer coefficient for the yawed cylinder to the value at zero yaw is plotted against yaw angle. This ratio $\bar{h}/\bar{h}_{\psi=0}$ was obtained by cross-plotting the data in figure 6 at the wall Reynolds numbers $\rho_\infty U_\infty D/\mu_w$ of 1.8×10^5 and 4×10^5, which correspond to the stream Reynolds numbers listed in figure 9. Data from references 5 and 6 at lower Reynolds numbers are included for comparison. The results of the present tests show that, at stream Reynolds numbers of about 15×10^5, the heat-transfer coefficient at 30° yaw is about twice the value at 0° yaw. As previously indicated by figure 8, this large increase in heat transfer is evidently caused by transition to turbulent flow followed by a forward movement of transition toward the stagnation line as the yaw angle is increased. Since the boundary layer is laminar at zero yaw, this forward movement of transition with yaw is obviously caused by some factor or combination of factors which change with yaw angle, such as a length Reynolds number or the three-dimensional nature of the flow (that is, the secondary flow) which occurs within the boundary layer as the cylinder is yawed. This latter effect has been previously observed and studied in detail on sweptback wings and rotating disks in references 12 and 13 and in investigations by Owen and Randall reported in papers of limited availability.

The heat transfer decreases by about 35 percent from the peak value for an increase in yaw angle from 35° to 60°, as shown in figure 9. This decrease apparently corresponds to the decrease in heat transfer with increasing yaw angle that would occur on a cylinder with a completely developed turbulent boundary layer, as indicated by the previous discussion concerning figure 8.

Effect of Yaw on Transition

Length Reynolds number.- In general there are perhaps two types of length Reynolds numbers which may characterize transition for a given set of circumstances. One of these length Reynolds numbers is based on the length from the leading edge measured along a streamline and the local stream velocity. In the case of a yawed flat plate this "streamwise" Reynolds number can be expected to have some significance. (See ref. 10.)

As an example, the transition data on a yawed flat plate (fig. 15 of ref. 11) is compared with predictions based on this type of Reynolds number, which may be defined as

$$R_{1_L} = \frac{\rho_1 V_1 L}{\mu_1}$$

where ρ_1, V_1, and μ_1 are taken as the local "effective" values outside the boundary layer. These local effective values may be calculated by assuming (as in ref. 23) that the flow near the surface, but outside the boundary layer, has gone through a normal shock (here computed for the component of the stream Mach number normal to the leading edge) corresponding to the shock from the leading edge and then reexpanded until the local static pressure on the plate is equal to the original stream static pressure. Thus, assuming that the value of R_{1_L} for transition is constant and equal to the value for zero yaw, the streamwise length from the leading edge to transition would be

$$\left(L_T\right)_\psi = \frac{\left(\frac{\rho_1 V_1}{\mu_1}\right)_{\psi=0}}{\left(\frac{\rho_1 V_1}{\mu_1}\right)_\psi} \left(L_T\right)_{\psi=0}$$

Then, using $\left(L_T\right)_{\psi=0} = 2.72$ inches from reference 11 results in the following values for the length of laminar run normal to the leading edge, $L_T \cos \psi$:

ψ, deg	$L_T \cos \psi$	
	Computed, in.	Experimental (ref. 10), in.
0	2.72	2.72
45	1.00	.86
50	.80	.70
55	.62	.57
60	.47	.43

The good agreement between the calculations and the experimental data indicates that the concept of streamwise Reynolds number, as defined here, can be used to determine the effect of yaw on transition on a flat plate.

This streamwise length Reynolds number loses much of its significance in flows with pressure gradient where the boundary-layer thickness and velocity profiles do not depend on the distance from the leading edge only. On a yawed blunt cylinder the length L along an external streamline cannot be defined if the starting point is taken as the stagnation line $(u_1 = 0)$ since L then becomes infinite, as can be seen from the expression for L, which may be written as

$$L = \int_0^x \frac{\sqrt{u_1^2 + U_\infty^2 \sin^2\psi}}{u_1} dx$$

This indicates that the flow in the neighborhood of the stagnation line is largely spanwise, and yet the boundary-layer thickness is constant and the velocity profiles are similar in this region. Thus, as is well known, a length Reynolds number for transition in this type of flow should be based on some local characteristic dimension of the boundary layer itself, such as the momentum thickness.

For incompressible flow on a yawed cylinder a "resultant" momentum thickness Δ may be defined as

$$\Delta = \int_0^\delta \frac{V}{V_1}\left(1 - \frac{V}{V_1}\right)dz$$

and a momentum-thickness Reynolds number is then defined as

$$R_\Delta = \frac{\rho V_1 \Delta}{\mu}$$

Then, from the method of reference 8, the momentum thickness was calculated for incompressible flow on a circular cylinder by using the equation

$$u_1 = 2U_{N_\infty} \sin\theta$$

for the chordwise velocity distribution. The local resultant velocity V_1 is then given by the expression

$$V_1 = \sqrt{4U_{N_\infty}^2 \sin^2\theta + U_\infty^2 \sin^2\psi}$$

The results of the calculation are summarized in the following table where the ratio $R_\Delta \sqrt{\frac{\rho U_\infty D}{\mu}}$ is given as a function of ψ and $\bar{x}$:

ψ, deg	$R_\Delta\sqrt{\frac{\rho U_\infty D}{\mu}}$ for -			
	$\bar{x} = 0.2$	$\bar{x} = 0.4$	$\bar{x} = 0.6$	$\bar{x} = 0.75$
0	0.11	0.22	0.34	0.46
20	.12	.22	.33	.45
40	.15	.22	.33	.43
60	.21	.27	.34	.43

These results indicate that the ratio $R_\Delta\sqrt{\frac{\rho U_\infty D}{\mu}}$ is almost independent of yaw angle for $\bar{x}$ greater than 0.4. Thus, if R_Δ has any significance as a parameter for transition on a cylinder, the value of the stream Reynolds number for transition should be about the same for all yaw angles. Since this is contrary to the experimental results of Bursnall and Loftin (ref. 9), who observed a decrease in the stream Reynolds number for transition $\left(\frac{\rho U_\infty D}{\mu}\right)_T$ from 3.7×10^5 to 2.1×10^5 for an increase in yaw angle from 0° to 60°, the parameter R_Δ apparently cannot be used to characterize the effect of yaw on transition on a cylinder in incompressible flow. This implies that some mechanism other than the Tollmien-Schlichting type of instability is present. Since the corresponding calculations of R_Δ for compressible flow have not yet been carried out, no definite conclusion as to the effect of viscous instability is possible for this case except for small yaw angles where the effects of compressibility would still be small.

Three-dimensional boundary-layer instability.- In an investigation by Owen and Randall a parameter χ which characterizes the stability of the boundary layer on a yawed cylinder or sweptback wing was defined as

$$\chi = \frac{\rho \delta v_{max}}{\mu} \tag{12}$$

where δ is the local boundary-layer thickness and v_{max} is the maximum velocity within the boundary layer in the direction perpendicular to the local external streamline. The velocity profile in this direction has an inflection point and is, therefore, dynamically unstable. An expression for χ in terms of the stream Reynolds number, yaw angle, and chordwise velocity distribution can be derived from an appropriate solution of the laminar-boundary-layer equations. For the incompressible case where the chordwise flow is independent of the spanwise flow this expression is

$$\frac{\chi}{\left(\frac{\rho U_\infty D}{\mu}\right)^{1/2}} = \frac{\sin\psi}{\sqrt{\cos\psi}\left[\left(\frac{u_1}{U_{N_\infty}}\right)^2 + \tan^2\psi\right]^{1/2}} F\left(\frac{u_1}{U_{N_\infty}}\right) \tag{13}$$

according to Owen and Randall, where $F\left(\frac{u_1}{U_{N_\infty}}\right)$ is a calculable function of $\frac{u_1}{U_{N_\infty}}$. From an analysis of wind-tunnel and flight-test results they showed that, when the value of χ reached approximately 125 on swept-back wings, characteristic streamwise striations were first observed in the agent used for visualizing transition (usually china clay). These striations were interpreted as the traces of small vortices (alined with their axes approximately parallel to the external stream) which, according to the analysis, are caused by the dynamic instability of the secondary flow. When χ reached about 175 the flow had become completely turbulent with transition moving forward to the neighborhood of the leading edge.

In order to compare these results for sweptback wings with the case of the yawed cylinder, equation (13) will be evaluated for a circular cylinder. The details of the method used by Owen and Randall for calculating F are not available; however, this function may be calculated from the integral method of reference 8 applied to incompressible flow. The result is

$$F\left(\frac{u_1}{U_{N_\infty}}\right) = C\lambda^{3/2}\frac{u_1}{U_{N_\infty}}\left(\frac{d}{d\bar{x}}\frac{u_1}{U_{N_\infty}}\right)^{-1/2} \tag{14}$$

where $C \approx 0.045$ by comparison with the approximate formula of Owen and Randall. Then, the use of $\frac{u_1}{U_{N_\infty}} = 2\sin\theta$ for the circular cylinder in equations (13) and (14) gives the expression

$$\frac{\chi}{\left(\frac{\rho U_\infty D}{\mu}\right)^{1/2}} = 0.045\frac{\sin\psi}{\sqrt{\cos\psi}}\lambda^{3/2}\sin\theta\left[\cos\theta\left(4\sin^2\theta + \tan^2\psi\right)\right]^{-1/2} \tag{15}$$

which is plotted against ψ in figure 10 for $\theta = 50^\circ$. The maximum value of the stability parameter χ_{max} occurred at $\theta \approx 50^\circ$ for all values of ψ. Using the values shown in figure 10 and the critical

Reynolds number for transition from reference 9 for a circular cylinder gives values of $\chi_T \approx 110$, 150, and 130 at $\psi = 30^\circ$, 45°, and 60°, respectively. These values of χ_T are in the same range as those of the Owen and Randall investigation, indicating that transition on the yawed circular cylinder in reference 9 is probably initiated by the same mechanism as on the sweptback wings.

Whether these values of χ can be used to predict the onset of instability or transition in compressible flow is not yet known, although data reported in reference 12 for a swept wing at $M_\infty = 1.61$ indicate that the instability occurs at a much lower Reynolds number than predicted by the Owen-Randall criterion. For purposes of comparison, a rough estimate of transition Reynolds numbers in the present tests can be obtained by extrapolating the data in figure 6 at 21° and 39.7° yaw back to the theoretical laminar lines for these yaw angles, and converting the "wall" Reynolds number $\rho_\infty U_\infty D/\mu_w$ to the stream Reynolds number $\rho_\infty U_\infty D/\mu_\infty$ These estimated values of transition Reynolds numbers are then compared in the following table with values predicted from equation (15) (or fig. 10) with $\chi_T = 130$ (as determined from the data of reference 9).

ψ, deg	$\frac{\chi_{max}}{\sqrt{\frac{\rho_\infty U_\infty D}{\mu_\infty}}}$ from figure 10	$\frac{\rho_\infty U_\infty D}{\mu_\infty}$ for $\chi_T = 130$	$\left(\frac{\rho_\infty U_\infty D}{\mu_\infty}\right)_T$ from figure 6
21.0	0.125	11.0×10^5	3.6×10^5
39.7	.220	3.5×10^5	1.8×10^5

The experimental values for the transition Reynolds numbers are seen to be about 1/3 to 1/2 of the values predicted by the stability parameter for incompressible flow. In reference 12 the experimental transition Reynolds number (not to be confused with the Reynolds number for the appearance of vortices) was about 1/10 of the predicted value, using $\frac{\chi_{max}}{R^{1/2}} = \frac{125}{\left(11.8 \times 10^6\right)^{1/2}} = 0.0363$ to correspond to their test conditions and using $\chi_T = 175$.

The above comparisons, together with the previous discussion on length Reynolds numbers, tend to indicate that the predominating cause of transition on a yawed cylinder is the inflectional instability of

the boundary layer. If this is the case, the transition Reynolds numbers obtained in the present tests (with tunnel turbulence and model roughness effects present) may reasonably be expected to be of the same order as corresponding values for free-flight conditions. Further evidence supporting this contention is that the inflectional instability of a three-dimensional boundary layer is very much more powerful than the viscous or Tollmien-Schlichting instability of a two-dimensional boundary layer, as shown in reference 13.

CONCLUSIONS

Experimental measurements of the average heat transfer on the forward half of a circular cylinder at a stream Mach number of 4.15 and stream Reynolds number range of 5×10^5 to 13×10^5 (based on cylinder diameter) resulted in the following general conclusions:

1. The average heat-transfer coefficients at zero yaw angle were in good agreement with values predicted by laminar theory and also correlated satisfactorily with other experimental results at lower Reynolds numbers.

2. At 35° yaw angle the heat-transfer coefficients were 50 percent to 100 percent higher than the values at zero yaw. This trend is in the opposite direction of that shown by previous data at lower Reynolds numbers where the heat-transfer coefficients at 35° yaw were about 20 percent lower than the values at zero yaw. The increase in heat transfer with increasing yaw angle, as observed in the present investigation, is attributed to transition from laminar to turbulent boundary layer which apparently occurred primarily as a result of the inflectional instability of the three-dimensional boundary layer on the yawed cylinder.

3. A further increase in yaw angle from 35° to 60° resulted in a decrease in heat-transfer coefficients (from the peak values) of about 35 percent. These data, when plotted in terms of typical turbulent correlation parameters, indicate that the magnitude of this decrease corresponds, approximately, to the decrease in heat transfer with increasing yaw angle that would be expected on a cylinder with a completely developed turbulent boundary layer.

4. The average recovery temperatures for zero yaw were in good agreement with the values predicted by laminar theory. The recovery temperatures at other yaw angles were between an upper limit corresponding to a theory for the turbulent boundary layer and a lower limit corresponding to a theory for the laminar boundary layer.

5. Estimates based on the results of the present investigation indicate that the Reynolds numbers (based on free-stream conditions and cylinder diameter) for transition on a yawed circular cylinder are about 4×10^5 and 2×10^5 for yaw angles of 20° and 40°, respectively, and for the Mach number and temperature conditions of the tests.

Langley Aeronautical Laboratory,
National Advisory Committee for Aeronautics,
Langley Field, Va., April 27, 1956.

REFERENCES

1. Jones, Robert T.: Effects of Sweep-Back on Boundary Layer and Separation. NACA Rep. 884, 1947. (Supersedes NACA TN 1402).

2. Sears, W. R.: The Boundary Layer of Yawed Cylinders. Jour. Aero. Sci., vol. 15, no. 1, Jan. 1948, pp. 49-52.

3. Goland, Leonard: A Theoretical Investigation of Heat Transfer in the Laminar Flow Regions of Airfoils. Jour. Aero. Sci., vol. 17, no. 7, July 1950, pp. 436-440.

4. Fluid Motion Panel of the Aeronautical Research Committee and Others: Modern Developments in Fluid Dynamics. Vol. II, ch. XIV, sec. 270, S. Goldstein, ed., The Clarendon Press (Oxford), 1938, p. 631.

5. Feller, William V.: Investigation of Equilibrium Temperatures and Average Laminar Heat-Transfer Coefficients for the Front Half of Swept Circular Cylinders at a Mach Number of 6.9. NACA RM L55F08a, 1955.

6. Goodwin, Glen, Creager, Marcus O., and Winkler, Ernest L.: Investigation of Local Heat-Transfer and Pressure Drag Characteristics of a Yawed Circular Cylinder at Supersonic Speeds. NACA RM A55H31, 1956.

7. Eggers, A. J., Jr., Hansen, C. Frederick, and Cunningham, Bernard E.: Theoretical and Experimental Investigation of the Effect of Yaw on Heat Transfer to Circular Cylinders in Hypersonic Flow. NACA RM A55E02, 1955.

8. Beckwith, Ivan E.: Theoretical Investigation of Laminar Heat Transfer on Yawed Infinite Cylinders in Supersonic Flow and a Comparison With Experimental Data. NACA RM L55F09, 1955.

9. Bursnall, William J., and Loftin, Laurence K., Jr.: Experimental Investigation of the Pressure Distribution About a Yawed Circular Cylinder in the Critical Reynolds Number Range. NACA TN 2463, 1951.

10. Emmons, H. W., and Bryson, A. E.: The Laminar-Turbulent Transition in a Boundary Layer. Proc. First U. S. Nat. Cong. Appl. Mech. (Chicago, Ill., 1951), A.S.M.E., 1952, pp. 859-868.

11. Dunning, Robert W., and Ulmann, Edward F.: Effects of Sweep and Angle of Attack on Boundary-Layer Transition on Wings at Mach Number 4.04. NACA TN 3473, 1955.

12. Scott-Wilson, J. B., and Capps, D. S.: Wind Tunnel Observations of Boundary Layer Transition on Two Sweptback Wings at a Mach Number of 1.61. Tech. Note Aero. 2347, British R.A.E., Dec. 1954.

13. Gregory, N., Stuart, J. T., and Walker, W. S.: On the Stability of Three-Dimensional Boundary Layers With Application to the Flow Due to a Rotating Disk. Phil. Trans. Roy. Soc. (London), Ser. A, vol. 248, no. 943, July 14, 1955, pp. 155-159.

14. Jakob, Max: Heat Transfer. Vol. 1, John Wiley & Sons, Inc., 1949, p. 275.

15. Eckert, E. R. G. (With appendix by Robert M. Drake, Jr.): Introduction to the Transfer of Heat and Mass. First ed., McGraw-Hill Book Co. Inc., 1950.

16. Squire, H. B.: Heat Transfer. Vol. II of Modern Developments in Fluid Dynamics - High Speed Flow, ch. XIV, L. Howarth, ed., The Clarendon Press (Oxford), 1953, pp. 757-853.

17. Kalikhman, L. E.: Heat Transmission in the Boundary Layer. NACA TM 1229, 1949.

18. Sommer, Simon C., and Short, Barbara J.: Free-Flight Measurements of Turbulent-Boundary-Layer Skin Friction in the Presence of Severe Aerodynamic Heating at Mach Numbers from 2.8 to 7.0. NACA TN 3391, March 1955.

19. Falkner, V. M.: A New Law for Calculating Drag. The Resistance of a Smooth Flat Plate With Turbulent Boundary Layer. Aircraft Engineering, vol. XV, no. 169, Mar. 1943, pp. 65-69.

20. Colburn, Allan P.: A Method of Correlating Forced Convection Heat Transfer Data and a Comparison With Fluid Friction. Trans. Am. Inst. Chem. Eng., vol. XXIX, 1933, pp. 174-210.

21. Penland, Jim A.: Aerodynamic Characteristics of a Circular Cylinder at Mach Number 6.86 and Angles of Attack Up to 90°. NACA RM L54A14, 1954.

22. Anon. (Compiled by F. C. Morey): The NBS-NACA Tables of Thermal Properties of Gases. Table 2.39 - Dry Air (Coefficients of Viscosity). Nat. Bur. Standards, Dec. 1950.

23. Moeckel, W. E.: Some Effects of Bluntness on Boundary-Layer Transition and Heat Transfer at Supersonic Speeds. NACA TN 3653, 1956.

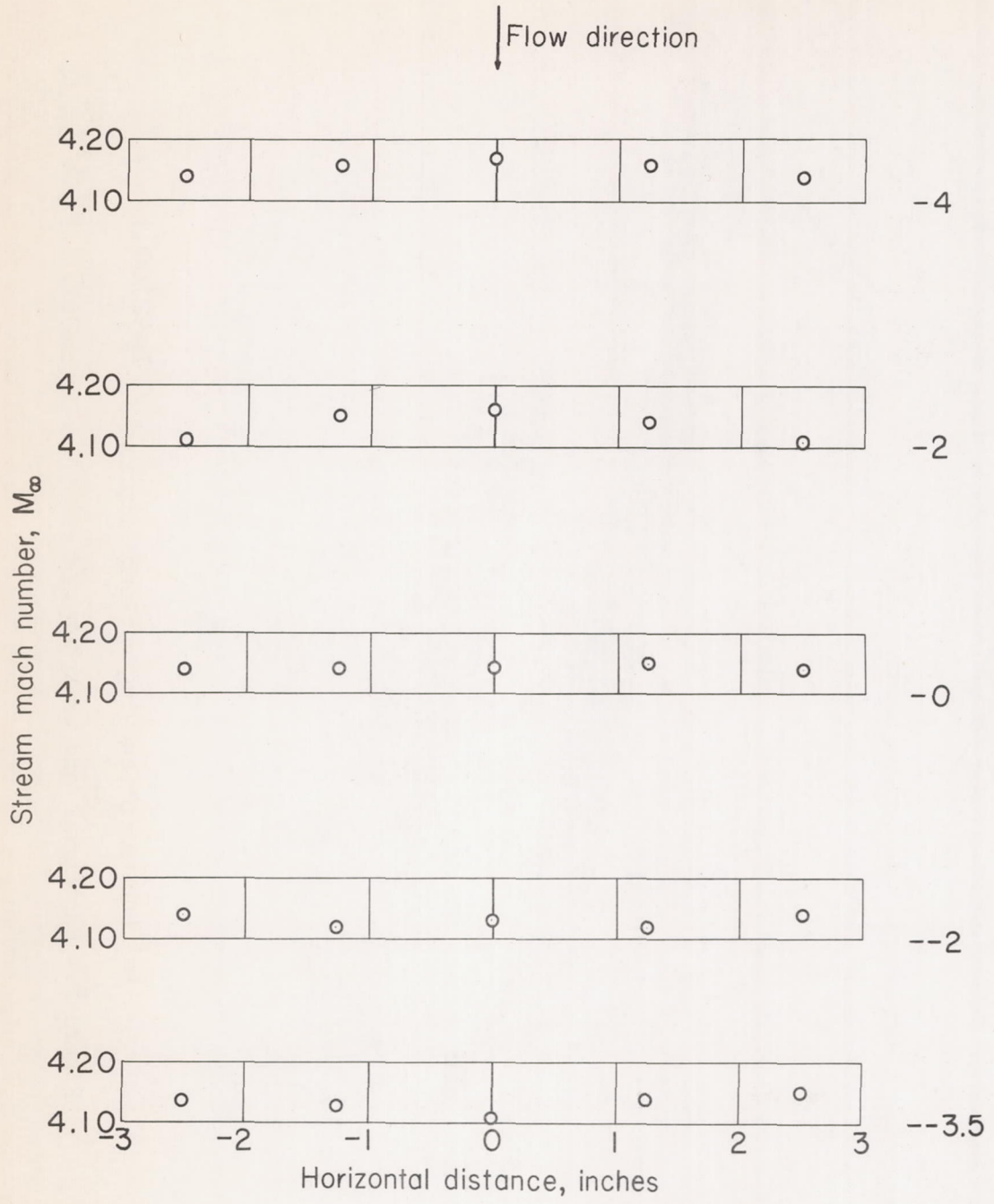
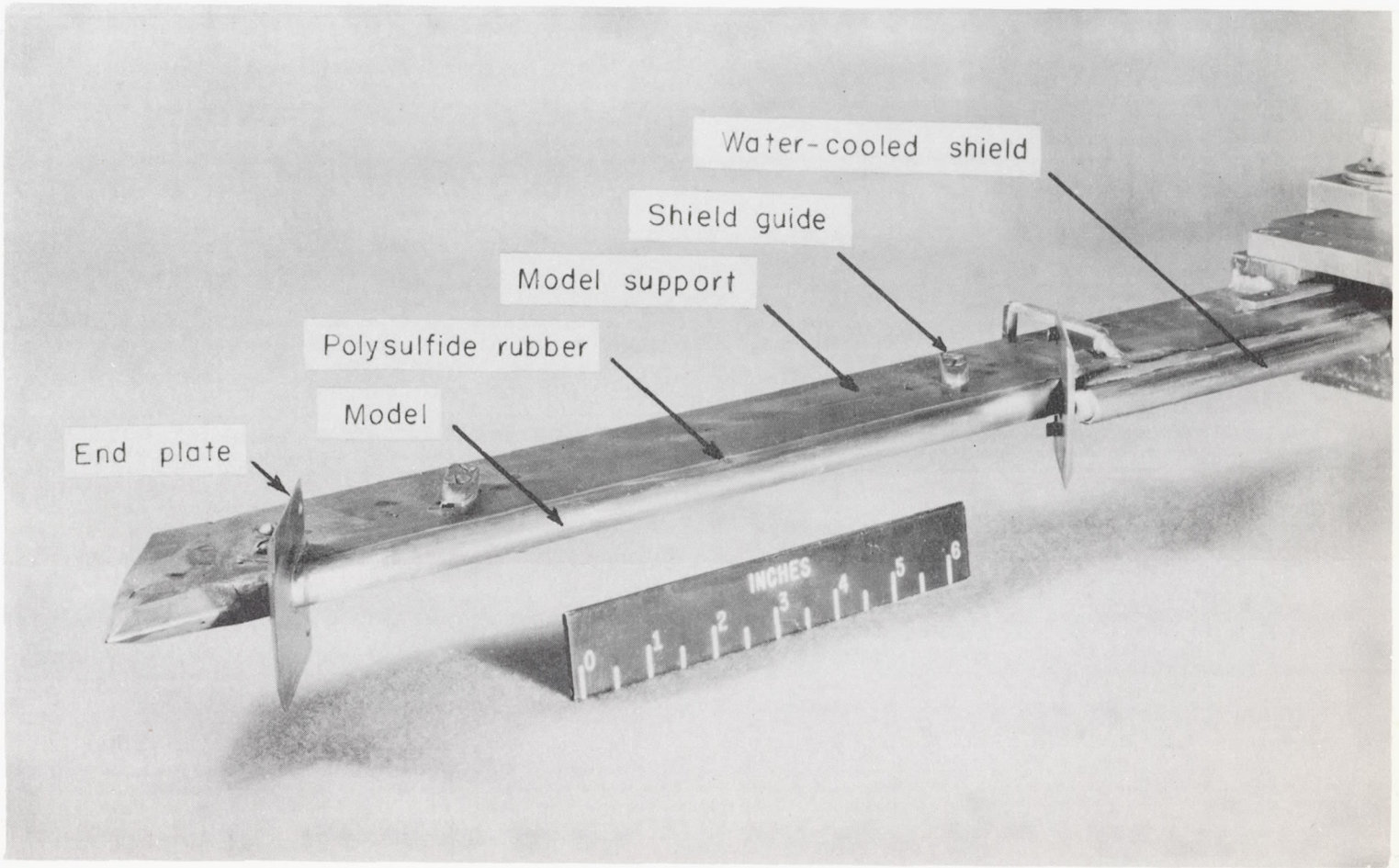
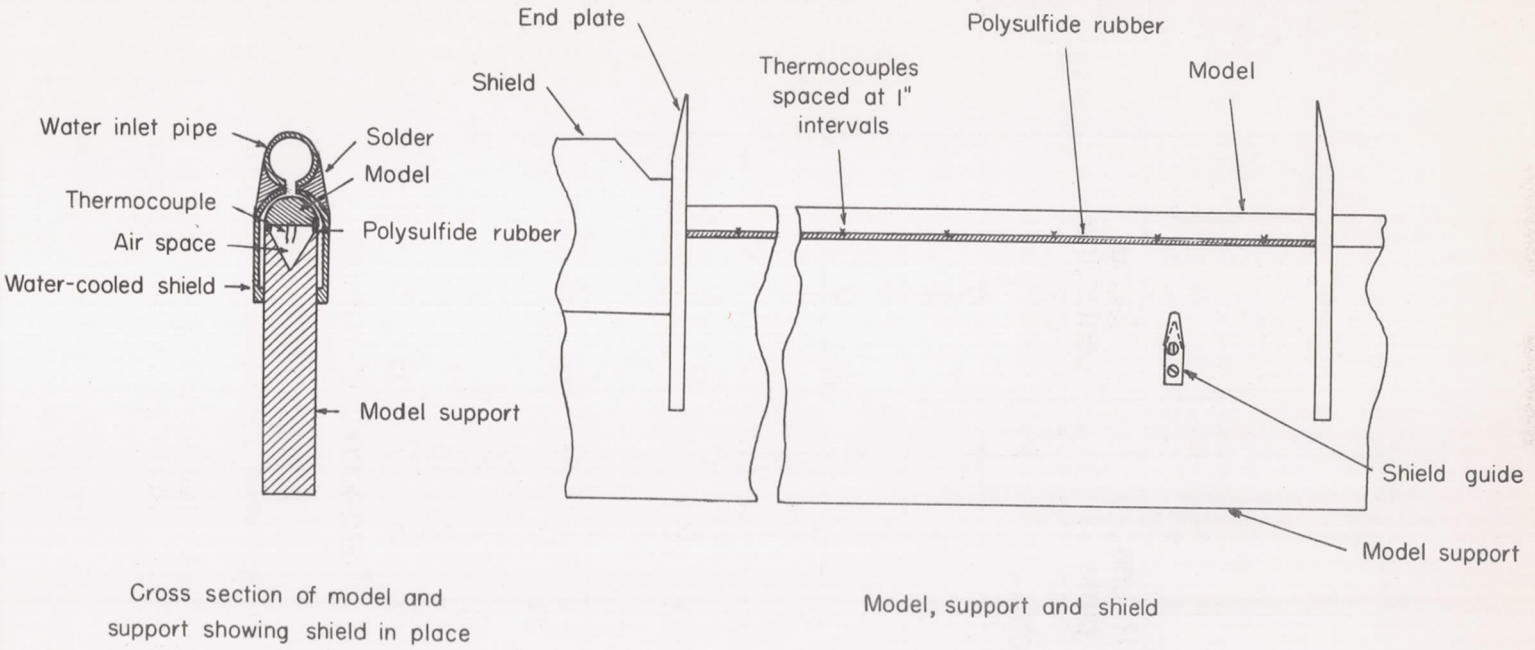


Figure 1.- Mach number distribution based on impact pressure measurements in the test region at 1/4 inch above the horizontal center plane.



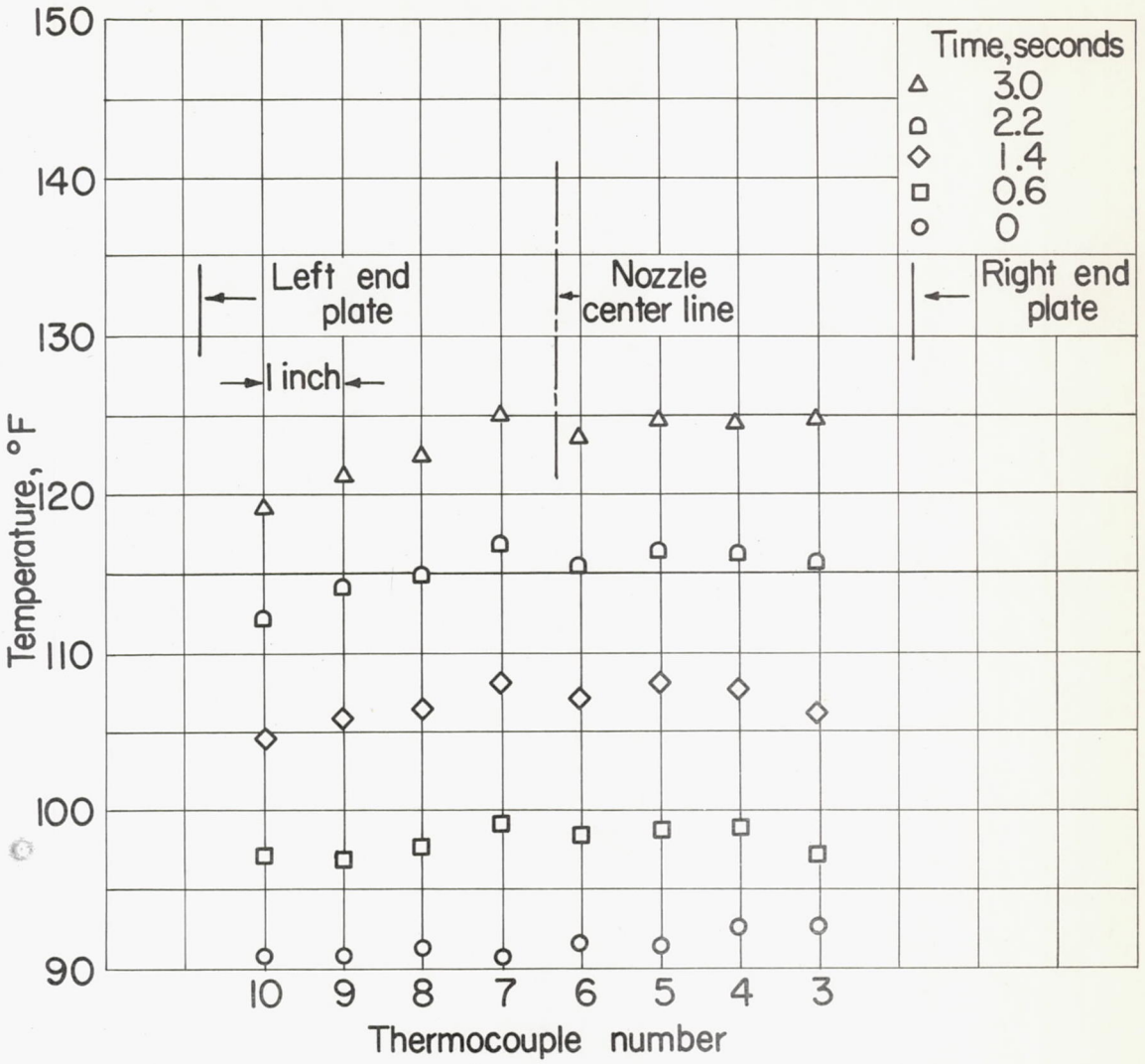
(a) Photograph showing various components. L-92100.1

Figure 2.- Photograph and sketches of heat-transfer model.



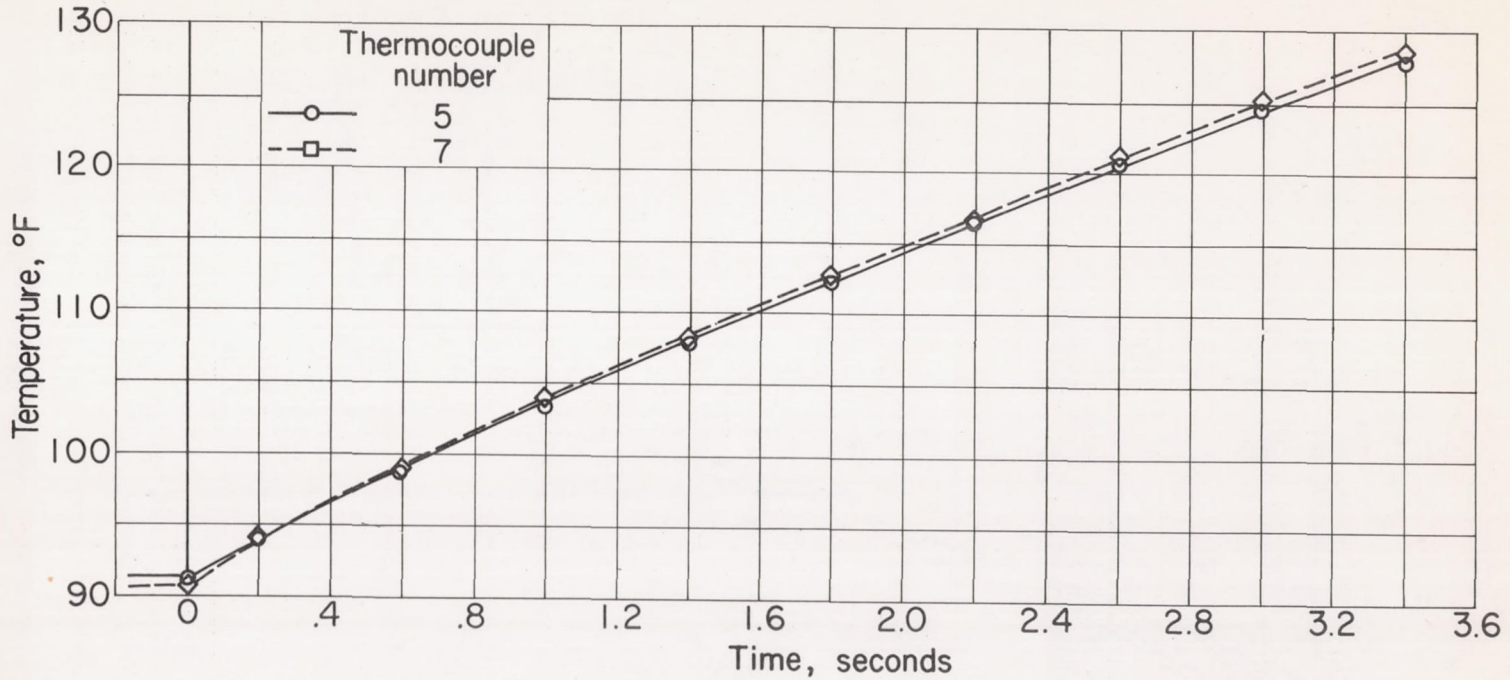
(b) Sketches of model.

Figure 2.- Concluded.



(a) Spanwise temperature distribution.

Figure 3.- Temperature time histories of the model for a typical run. $\psi = 0^{\circ}$; p_o = 411 pounds per square inch gage; $T_o = 249^{\circ}$ F.



(b) Temperature variation with time at two stations on the model.

Figure 3.- Concluded.

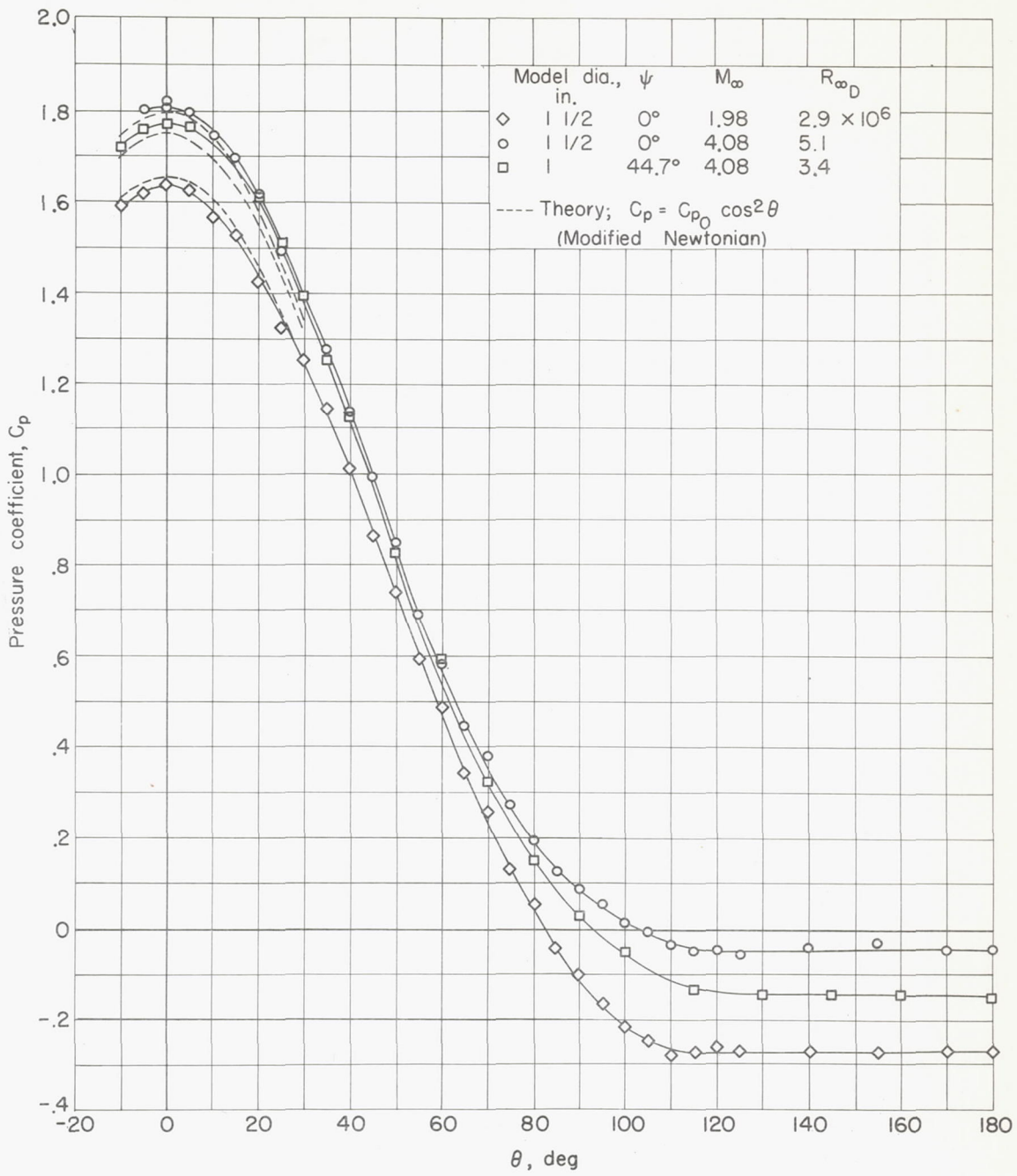


Figure 4.- Chordwise variation of the crossflow pressure coefficient on circular cylinders. The theoretical values of C_{p_o} were computed from the normal-shock equations for the corresponding experimental conditions.

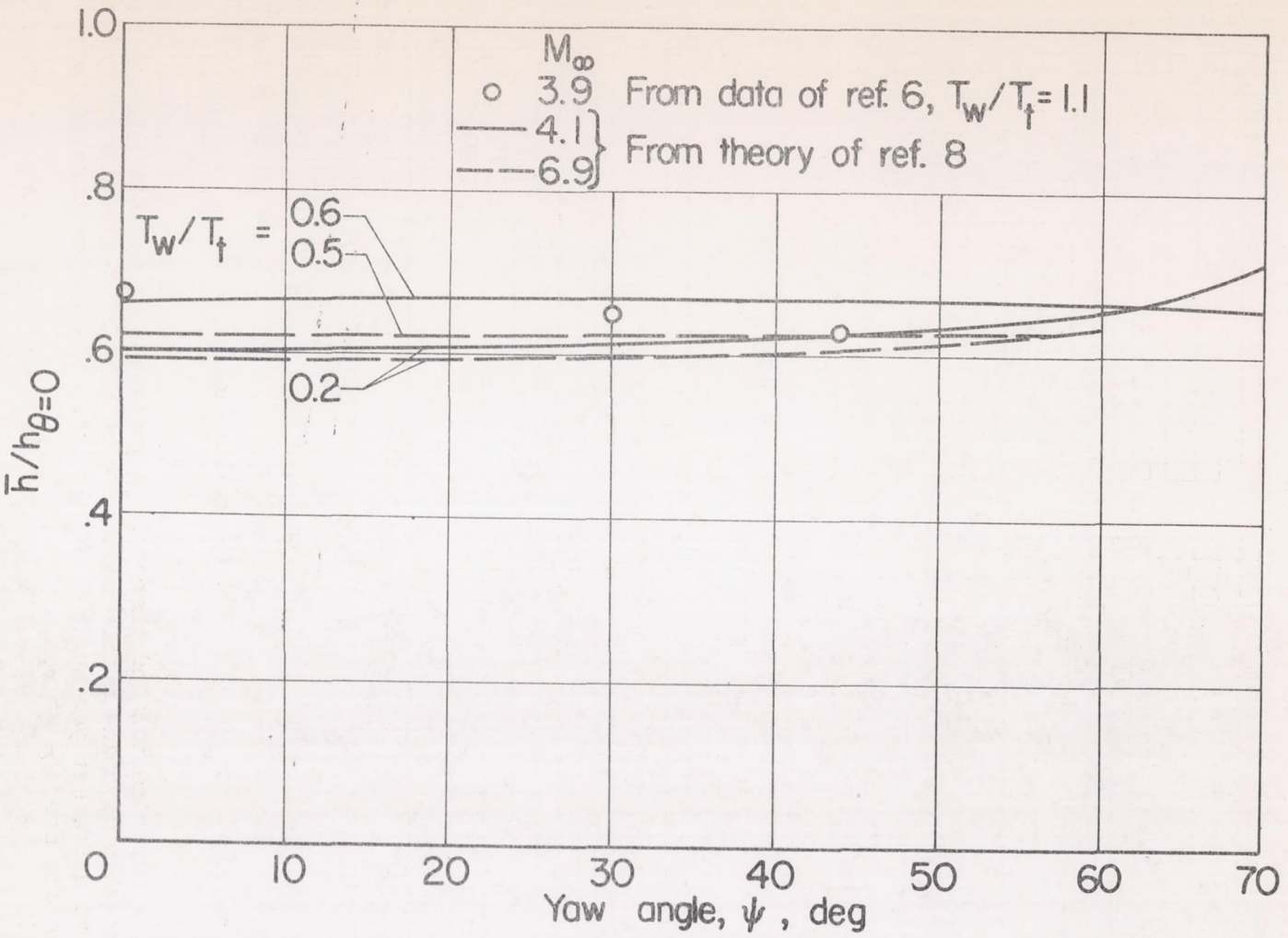


Figure 5.- Comparison of theory and experiment for the ratio of the average heat-transfer coefficient on the front half of a yawed cylinder to the alue at the stagnation line.

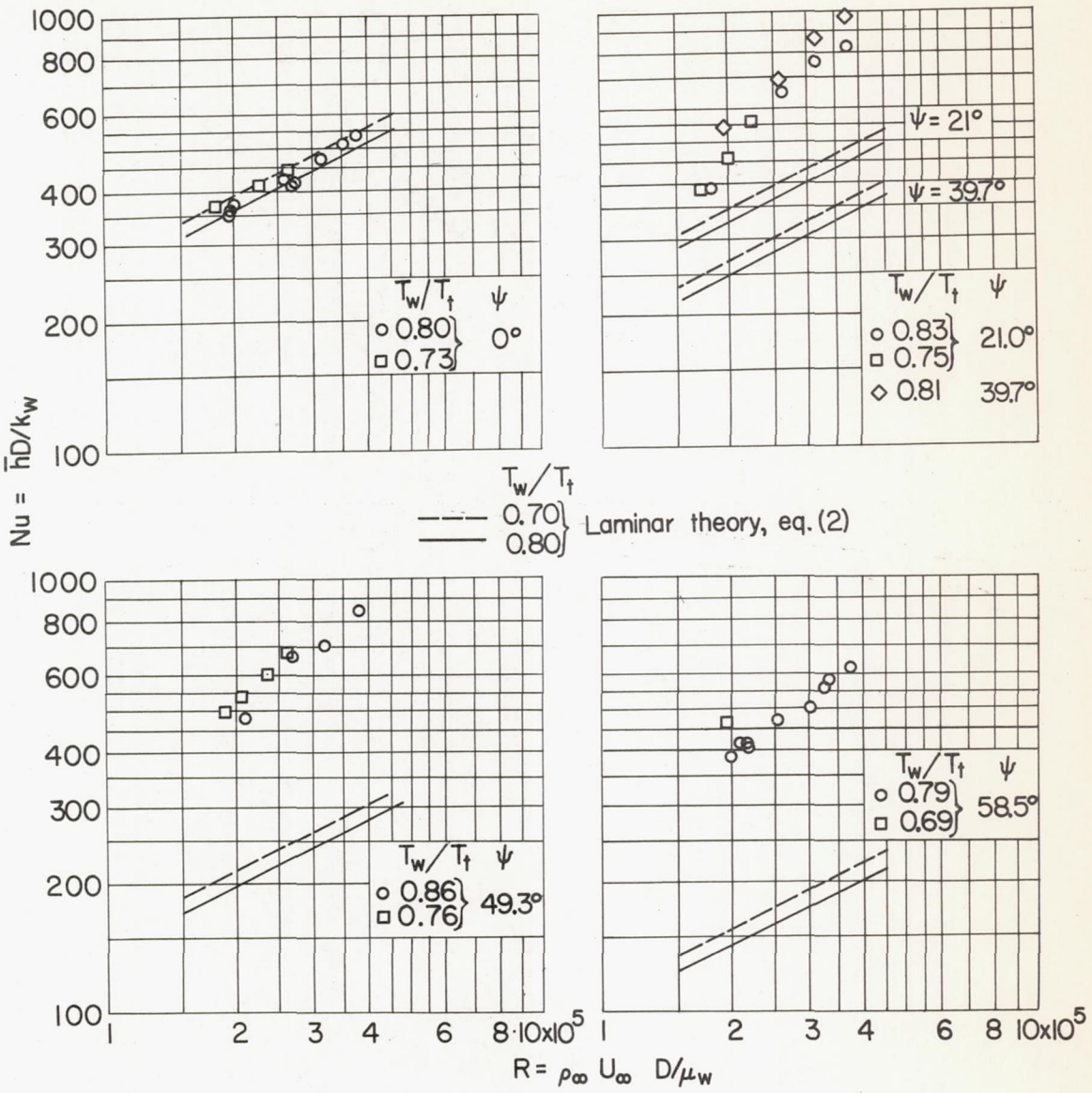


Figure 6.- Experimental and theoretical variation of average Nusselt number with Reynolds number on the front half of a circular cylinder at five different yaw angles. $M_\infty = 4.15$. The temperature ratios listed are average values.

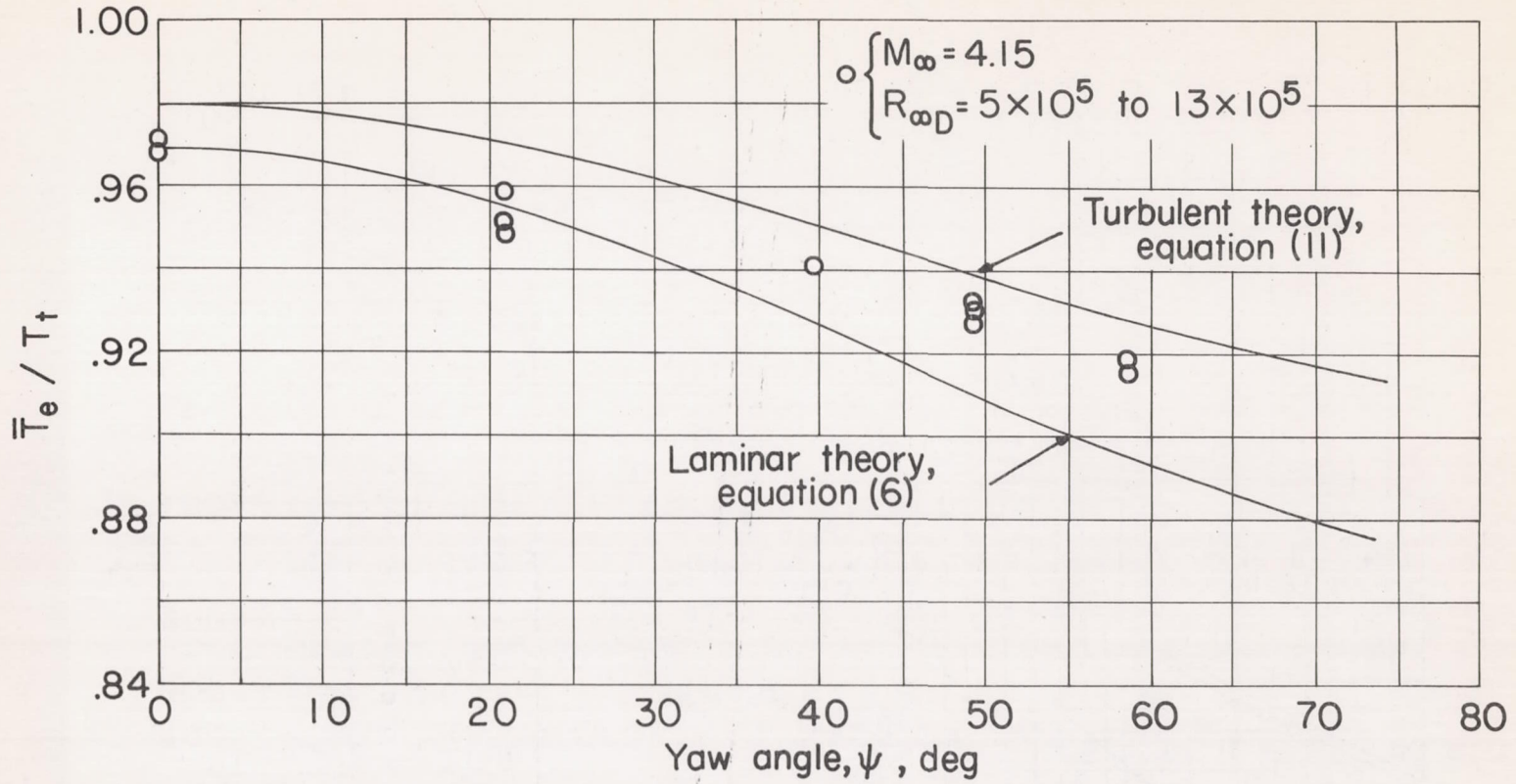


Figure 7.- Experimental and theoretical variation of average recovery-to-stagnation temperature ratio on the front half of a circular cylinder. Values used in the theory were $M_\infty = 4.15$ and $\sigma = 0.7$.

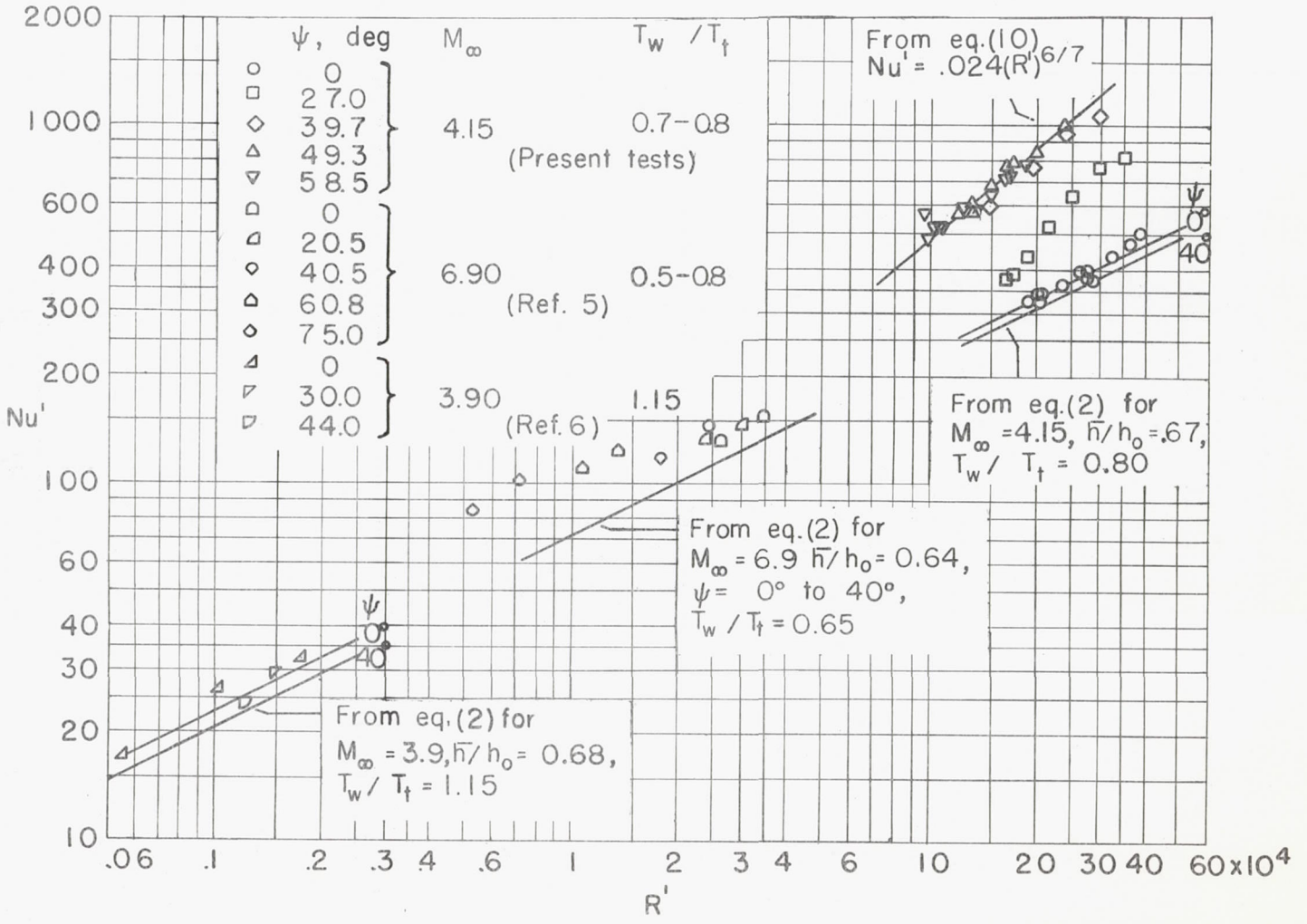


Figure 8.- Comparison of the average heat-transfer coefficients in terms of correlation parameters on the front half of a circular cylinder at different flow conditions and yaw angles.

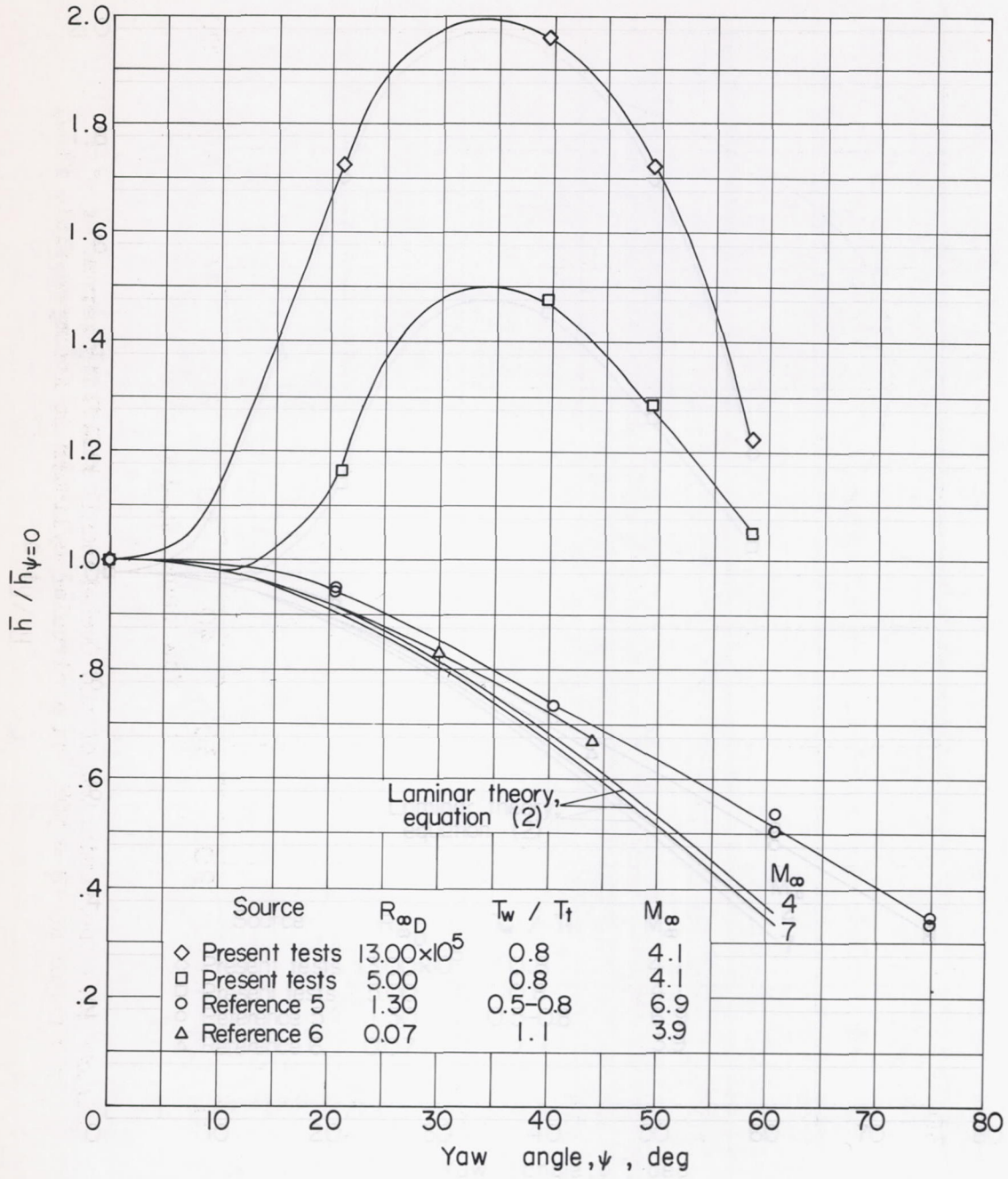


Figure 9.- Effect of yaw angle and Reynolds number on the ratio of the average heat-transfer coefficient on the front half of a yawed cylinder to the value at zero yaw.

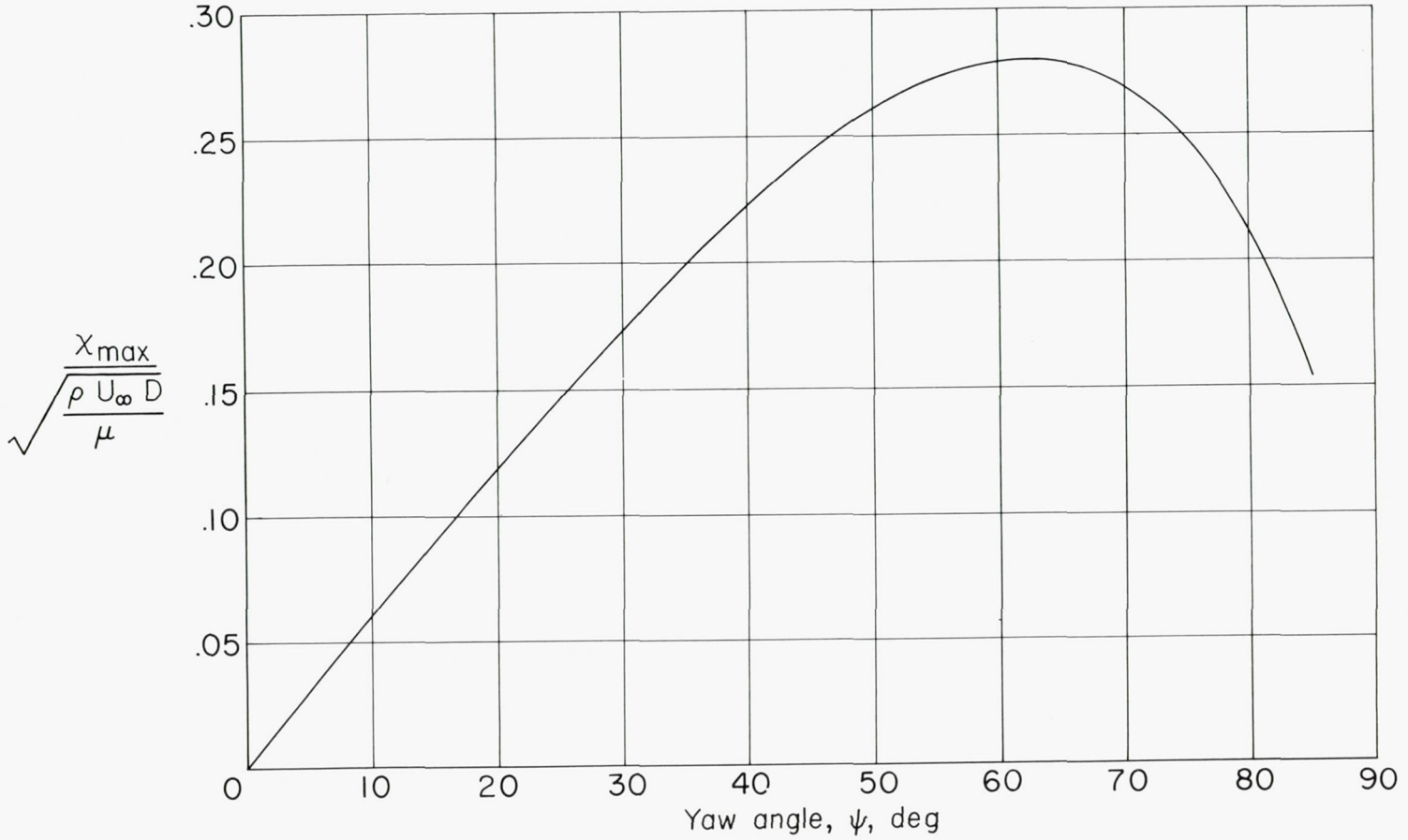


Figure 10.- The variation of the Owen-Randall stability parameter with yaw angle at $\theta = 50^\circ$ on a circular cylinder in incompressible flow.

NACA - Langley Field, Va.